Multi-decadal Satellite Gravity Mission Simulations Comparing Resolving Capabilities of a Long-term Trend in the Global Ocean Heat Content

Marius Schlaak[1*], Roland Pail[1], Alejandro Blazquez[2], Benoit Meyssignac[2], and Jean-Michel Lemoine[3]

[1] Technical University of Munich, TUM School of Engineering and Design, Chair for Astronomical and Physical Geodesy, Munich, German

[2] LEGOS, Université de Toulouse, CNES, CNRS, IRD, UPS, 31400 Toulouse, France

[3] GET, Université de Toulouse, CNES, CNRS, IRD, UPS, 31400 Toulouse, France

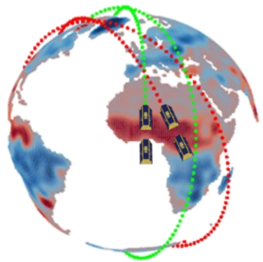

*contact me via email, LinkedIn, ResearchGate

EGU23, Vienna
On-site Poster Presentation
EGU23-8590, X2.56

EGU General Assembly 2023

IAPG

1.1 Measuring global ocean heat content as a proxi for the Earth Energy Imbalance

- Changes in Ocean Heat Content (**OHC**) represents good proxy for Eath Energy Imbalance (**EEI**), as the ocean absorbs more than 90% of EEI.
- The signal magnitude of EEI is small compared to incoming energy from solar radiation.
- EEI at the top of the atmosphere causes energy to accumulate in the Earth's system and drives climate change

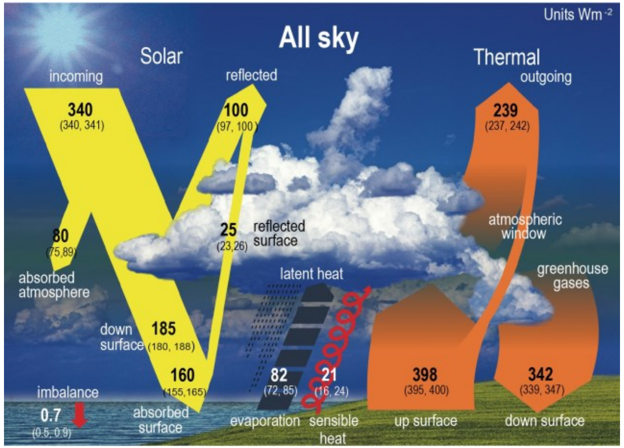

Fig. 1: Global energy budget of the Earth beginning of 21st century. The magnitude of the globally averaged components is given in Wm^{-2} (from Forster et al. 2021).

LEGOS Géosciences Environnement Toulouse cnes Centre National d'Études Spatiales

- Space geodetic techniques allow global measurements of the thermal extension of the oceans using the Sea Level (**SL**) budget equation

(Eq.1) $\Delta SL_{total} = \Delta SL_{mass} + \Delta SL_{thermo} + \Delta SL_{halo}$

- Globally the change in salinity in the oceans in negligible, therefore, Eq.1 can be simplified to get the thermosteric SL change

(Eq.2) $\Delta SL_{thermo} = \Delta SL_{total} - \Delta SL_{mass}$

- With an expansion coefficient (ε) changes in OHC can be derived (Eq.3).

(Eq.3) $\Delta OHC = \frac{\Delta SL_{thermo}}{\varepsilon}$

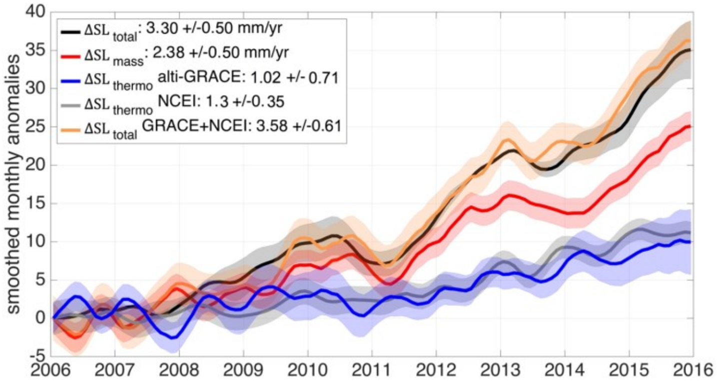

Fig. 2: Global mean anomalies of global mean sea level, including ΔSL_{total} in black, and its components (ΔSL_{mass}) in red and ΔSL_{thermo} in blue (from *[2]*).

2. Measuring ocean heat content with space geodetic techniques

- Total SL changes (ΔSL_{total}) are measured with satellite altimetry
- Current altimeter data measures a SL trend of $\Delta SL_{total} = 3.54 \pm 0.4$ mmyr^{-1} *[1].*
- Mass component of SL change (ΔSL_{mass}) is determined by satellite gravity missions.
- Current GRACE estimations quantify the mean mass component of the sealevel rise to be ΔSL_{mass} : 1.83 ± 0.21mmyr-1 *[1]*.

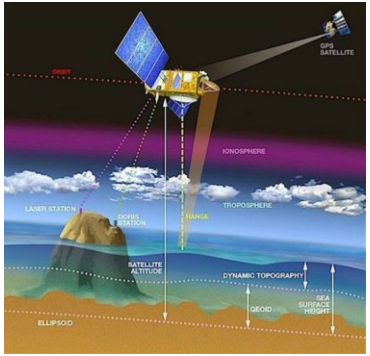

Fig. 3: Satellite altimetry range measurement of sea level (credit; CLS, AVISO)

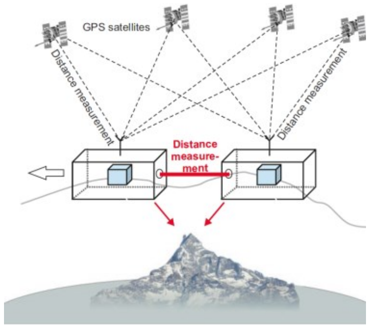

Fig. 4: Satellite Gravimetry principle using Satellite-Satellite-Tracking measurements. (from Angermann et al. 2022)

3. Climate model projections to evaluate improvements of future satellite gravity missions

- Model input is based on mean CMIP6 esemble projections
- Offline models provide estimates of ice sheet and glacier melting according to the CMIP projection
- Challenging difference in magnitudes over land compared to sea:
  - Decimeter per year on the continents
  - Millimeter per year in the oceans
- Model data from 2016 to 2100 (d/o 170) is used

What improvements in accuracy of ΔOHC can be expected from the Mass change And Geosciences International Constellation (MAGIC)?

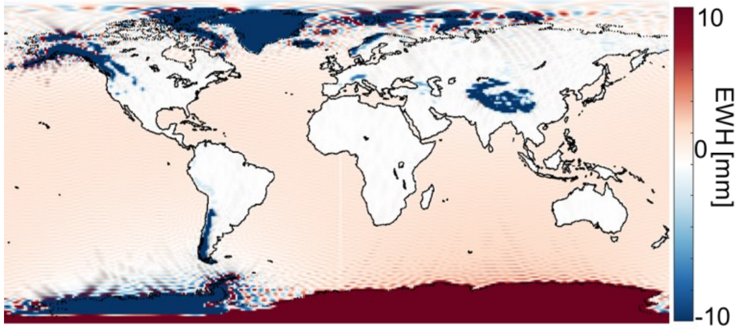

Fig. 5: Climate model data in mm EWH after spherical harmonic analysis to d/o 170. Example for 2016.

4.1 Closed loop simulations of future satellite gravimetry observation concept (MAGIC)

Input signals (d/o 80):

- GFDL-CM4 →SSP 5-8.5 Ice sheets, Glacier and Ocean signals
- OT-error → Model difference EOT11a-GOT4.7

Instrument Noise (MAGIC):

- Accelerometer $\mathrm{ACC_{LoS}} = 1 \cdot 10^{-11} \sqrt{\frac{\left(\frac{0.001\mathrm{Hz}}{\mathrm{f}}\right)^2}{\left(\left(\frac{0.00001\mathrm{Hz}}{\mathrm{f}}\right)^2 + 1\right)} + 1 + \left(\frac{\mathrm{f}}{0.1\mathrm{Hz}}\right)^4}$ $\left[\frac{m}{s^2\sqrt{Hz}}\right]$

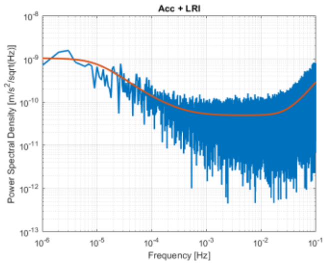

- LRI (polar) $\mathrm{LRI_{GFO}} = \sqrt{\left(\mathrm{L} \cdot \frac{10^{-15}}{\sqrt{\mathrm{f}}}\right)^2 + \left(\frac{10^{-12}}{\mathrm{f}^2}\right)^2}$ $\left[\frac{m}{\sqrt{Hz}}\right]$
- LRI (inclined) $\mathrm{LRI} = \mathrm{L} \cdot \left(2 \cdot 10^{-13} \sqrt{1 + \left(\frac{0.01Hz}{f}\right)^2} \sqrt{1 + \left(\frac{0.001Hz}{f}\right)^2}\right)$ $\left[\frac{m}{\sqrt{Hz}}\right]$

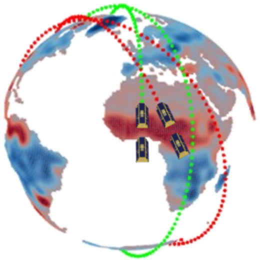

Orbits:

- Polar pair: 5-day sub-cycle at **high** altitude (p_5d_H)
- Inclined pair: 5-day sub-cycle at **mid** altitude (i_5d_Mb)
- Orbits repeat every 30 days at a 5s sampling.

4.2 Closed loop simulations of future satellite gravimetry observation concept (MAGIC)

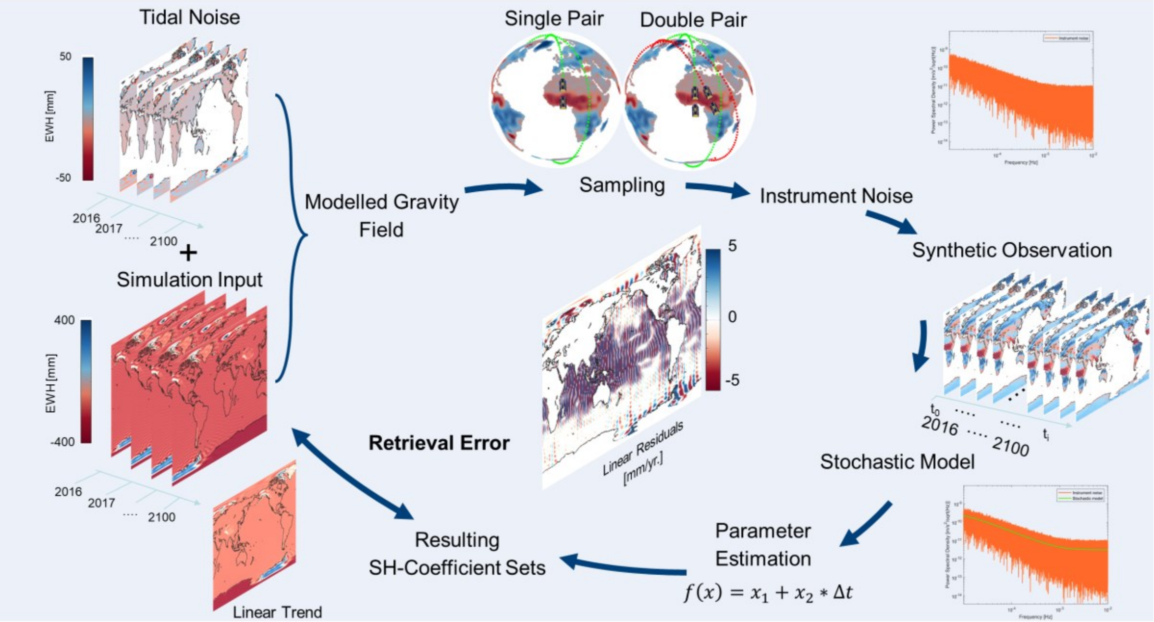

Fig. 6: Numerical closed loop simulation environment for single pair and double pair simulations following the MAGIC baseline scenario.

5.1 Simulation results

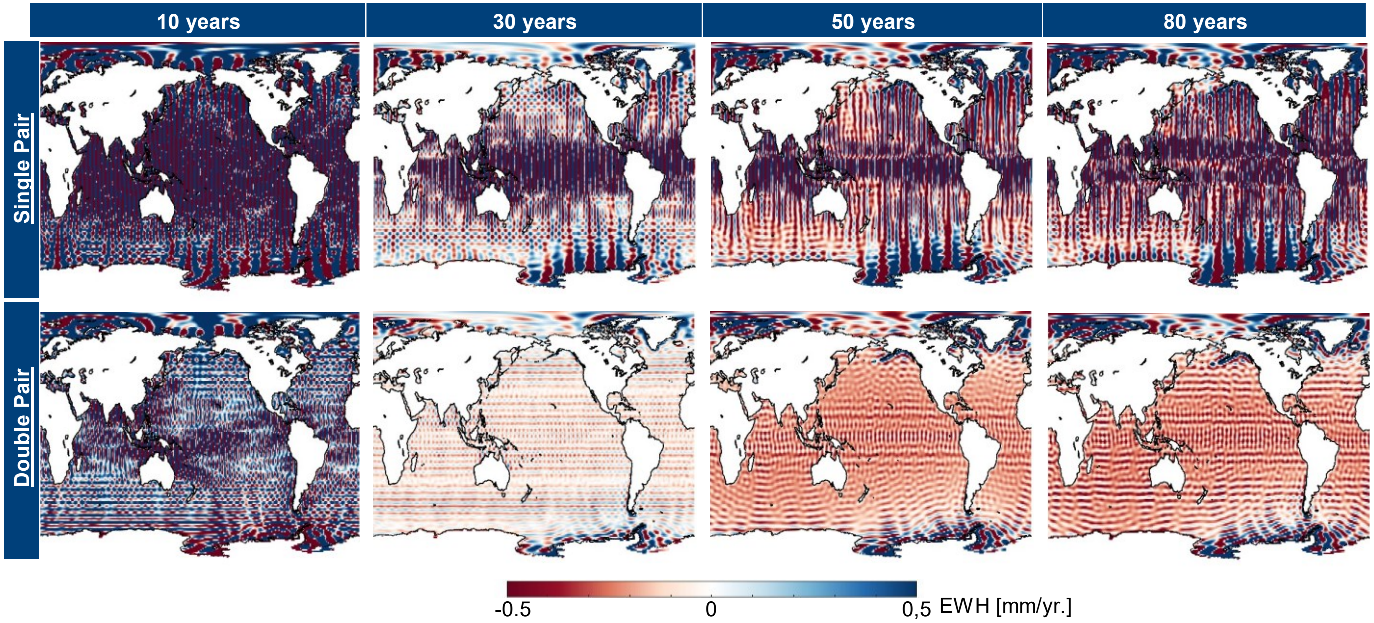

Fig. 7: Residuals for linear trend estimation from single (upper row) and double pair (lower row) simulations considering (from left to right) 10, 30, 50, 80 years of observations given in EWH [mmyr^{-1}].

- Improved long-term trend (Fig. 7) with:
  - Increased observation period
  - Advanced observation system
- Aliasing errors are strongest in polar regions

5.2 Simulation results

- CMIP6 model data shows an acceleration of sea-levelrise over the century
- Excluding polar areas, the ocean RMS reduces even further to 1 $mmyr^{-1}$ for the single pair and 0.2 $mmyr^{-1}$ for the double pair (Table 1).
- After a couple of years OT-aliasing is no more reduced by the increased number of observations, due to the fixed orbit repeat pattern.
- The residuals show a minimum, after 30 years.
- The increase in residuals after 30 years is correlated with the accelerated ice loss increasing the Gibbs effect.

	Reference	Single Pair	Double Pair
[yrs.]	Mean ΔSL_{mass} [mm/yr.]	Ocean RMS [mm/yr.]	Ocean RMS [mm/yr.]
10	1.16	7.76	0.86
30	1.85	0.98	0.13
50	2.44	0.91	0.22
80	3.76	0.97	0.26

Table 1. Mean ocean trend computed between latitudes $\lambda = \begin{cases} < +70 \\ > -70 \end{cases}$ and the corresponding root mean square error of the residuals over the ocean for single and double pair for the time intervals 10, 30, 50, and 80 years.

6. Outlook & Conclusion

- The simulation environment allows realistic estimation of satellite gravity observations for GRACE-FO and MAGIC constellation for Spherical Harmonic (SH) degree 80. In future work it is planned to increase the maximum degree and order to 160.
- Large difference in the input signal magnitude between continents and ocean causes Gibbs phenomena in the SH representation, especially in regions of intense and localized signals.
- Post-processing of simulation results is still to be done. As well as the computation of the thermosteric sea-level change ΔSL_{thermo} to evaluate the gain in accuracy that is to be expect from MAGIC for the assessment of EEI.
- MAGIC already shows a clear improvement in RMS estimating ΔSL_{mass} especially in the areas covered by the inclined pair between the latitudes -70 and 70.

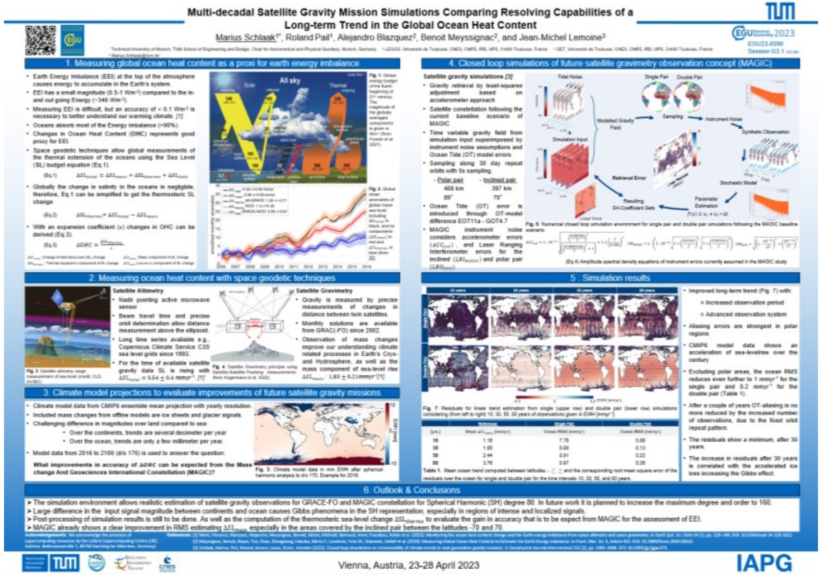

LEGOS
GÉOSCIENCES ENVIRONNEMENT TOULOUSE
cnes CENTRE NATIONAL D'ÉTUDES SPATIALES

References

[1] Marti, Florence; Blazquez, Alejandro; Meyssignac, Benoit; Ablain, Michaël; Barnoud, Anne; Fraudeau, Robin et al. (2022): Monitoring the ocean heat content change and the Earth energy imbalance from space altimetry and space gravimetry. In *Earth Syst. Sci. Data* 14 (1), pp. 229–249. DOI: 10.5194/essd-14-229-2022.

[2] Meyssignac, Benoit; Boyer, Tim; Zhao, Zhongxiang; Hakuba, Maria Z.; Landerer, Felix W.; Stammer, Detlef et al. (2019): Measuring Global Ocean Heat Content to Estimate the Earth Energy Imbalance. In *Front. Mar. Sci.* 6, Article 432. DOI: 10.3389/fmars.2019.00432.

[3] Schlaak, Marius; Pail, Roland; Jensen, Laura; Eicker, Annette (2022): Closed loop simulations on recoverability of climate trends in next generation gravity missions. In Geophysical Journal International 232 (2), pp. 1083–1098. DOI: 10.1093/gji/ggac373.

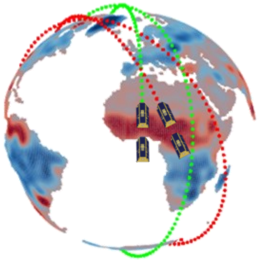

Marius Schlaak: email, LinkedIn, ResearchGate

EGU23, Vienna
On-site Poster Presentation
EGU23-8590, X2.56